MATHEMATICAL BIOSCIENCES
AND ENGINEERING
Volume **5**, Number **3**, July **2008**

http://www.mbejournal.org/

pp. **549–565**

AN EXTENSION OF THE BERETTA-KUANG MODEL OF VIRAL DISEASES

Ivo Siekmann, Horst Malchow

Institut für Umweltsystemforschung
Universität Osnabrück, Germany

Ezio Venturino

Dipartimento di Matematica
Università di Torino, Torino, Italy

(Communicated by Edoardo Beretta)

Abstract. A model for the complete life cycle of marine viruses is presented. The Beretta-Kuang model introduces an explicit equation for viral particles but the replication process of viral particles in their hosts is not considered. The extended model keeps the structure of the original model. This makes it possible to estimate the growth parameters of the viruses for a given parametrisation of the Beretta-Kuang model.

1. **Introduction.** During recent years, strong efforts have been made to model viral infections in plankton populations; usually the infection has been modelled by a contact rate of susceptibles and infected phytoplankton, [5], [2] and [3]. In these articles a predator feeding on the phytoplankton also has been considered. Beretta and Kuang included an explicit equation for viral particles in an infection model of phytoplankton without considering a predator [1].

In [8], this model was extended by a predator so that a combination of both ideas, the modelling of a prey-predator system with infected prey and the explicit consideration of viruses rather than modelling the infection by contacts of susceptibles and infected, was achieved.

Another extension of the model proposed in [1], which will be presented in this article, is to take a closer look at the process of viral replication. Beretta and Kuang considered only free viral particles. The replicating viruses which are confined in their hosts and which are set free again when the host dies from the infection are not taken into account.

The aim of the model presented here is to give a more complete description of the life cycle of viruses. In [1], free viruses "disappeared" in their hosts with a rate λSV and "reappeared" at the time of lysis. However, in this extension of [1], as the total population of hosts, P_H, consists of the two disjoint subpopulations of susceptibles S and infected I; the total virus population P_V is also subdivided among free viruses, V, and viruses confined in hosts, W. Therefore the virus population can be computed by summing up free and confined viruses, $P_V = V + W$

2000 *Mathematics Subject Classification.* Primary: 92B05, 37N25; Secondary: 37G10.
Key words and phrases. lytic viral infection, viral replication, Hopf bifurcation.
Work supported by a grant of the Vigoni program, DAAD-CRUI.

as the phytoplankton population is obtained by summing susceptibles and infected. Figure 1 shows a scheme of both models.

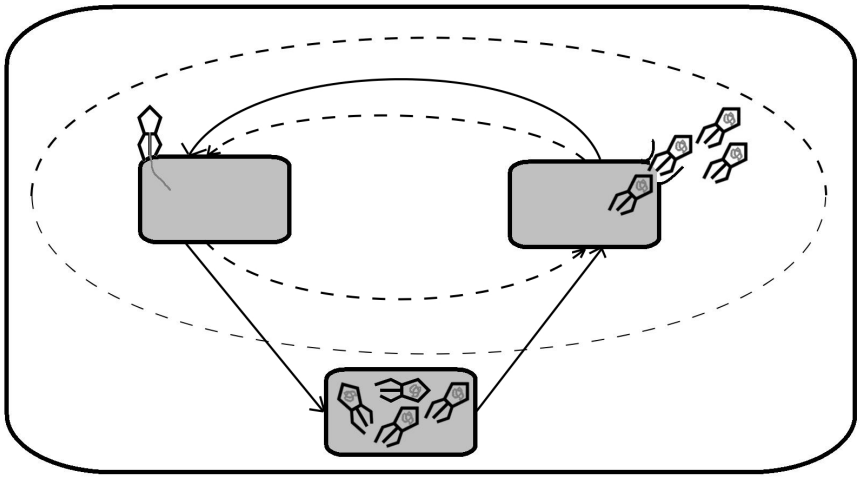

FIGURE 1. Schematic representation of the model by Beretta and Kuang [1] and of the extension. The original model is shown in the dashed ellipse, modelled processes are represented by dashed arrows, whereas the extension is displayed in the solid rectangle, modelled processes are indicated by solid arrows here. It shows that infection and lysis are already represented in the original model whereas viral replication in the host cells is considered explicitely only in the extension.

2. **A simple model for virus replication in hosts.** First, a short look shall be taken at the original model, [1].

$$\begin{aligned} \frac{dV}{dt} &= -\lambda SV - m_V V + Bm_I I, \\ \frac{dS}{dt} &= -\lambda SV + rS\left(1 - \frac{S+I}{K}\right), \\ \frac{dI}{dt} &= \lambda SV - m_I I. \end{aligned} \tag{1}$$

Here λ denotes the contact rate between susceptibles and viral agents, m_V the virus mortality, m_I the disease-related mortality for the host population, r the net reproduction rate, assuming that only sound individuals reproduce and their offspring are also sound at birth. K is the environment's carrying capacity for the population in question. We assume thus logistic growth, taking into account that infected individuals contribute to the population pressure term of the susceptibles.

Because we will add an equation for viruses W which are confined in their hosts, the equations of susceptibles and infected will not change. There will also be only a small change in the equation describing free viruses V: the amount of replicated viruses which are set free at the time of lysis will not be a constant parameter B as

in (1). As B is defined as the average number of viruses which are set free at the moment when a host cell dies we choose

$$B = \epsilon \overline{W} := \epsilon \frac{W}{I} \tag{2}$$

where $\overline{W}$ is the average of viruses confined in each cell and ϵ is a positive number above 1; this accounts for the fact that more viruses than the average might be released, because it is more likely that an infected host cell dies if it contains more viruses than the average. However, the authors believe that ϵ should not be very far from 1: If the total number of viruses W is only slightly above I, for most possible combinations, most of the host cells contain the average amount of viruses (which in this case is slightly above 1). Thus, a low value for $\overline{W}$ indicates that the infection is at an early stage, which means that most of the hosts have only recently been infected and the replication process has just started. Therefore, in this case it is justifiable to assume that the viruses are distributed uniformly over the infected host cells. However, the dynamics of the infection process provides another mechanism which justifies the assumption of a *uniform distribution* of viruses over host cells also for later stages of the infection; i.e., for higher values of $\overline{W}$, if a single host cell contains more viruses than the average amount $\overline{W}$ of viruses, then it should be more likely to die by lysis than would the hosts which contain $\overline{W}$ or less. As in most of the possible distributions of W viruses over I infected host cells, the majority of the cells contain less than the average $\overline{W}$; this mechanism decreases the deviation from a uniform distribution, because the fewer hosts which contain more viruses than the average disappear by lysis. Thus, in the case that $\overline{W}$ is far from 1, the assumption of a uniform distribution of viruses over host cells also seems to be a good approximation.

Furthermore, the above analysis shows that the mortality m_I shall be regarded as an average value. If the infection is at an early stage, a constant value m_I overestimates the mortality of infected. On the other hand, m_I should drop suddenly when several hosts die by lysis as the average amount of viruses per hosts is decreased. Therefore the model can only be appreciated accurately if it is regarded as a statistical model—the solutions of the deterministic extension of the model (1) shall be understood as average values of the population levels, averaged in time as well as over stochastic variations of the populations.

However, the authors prepare an extension of the model where m_I is no longer constant but depends on the average value $\overline{W}$ of viruses per host, to make the model more realistic. We can now state the equations for V and W:

$$\frac{dV}{dt} = -\lambda SV - m_V V + \epsilon \overline{W} m_I I, \tag{3}$$

$$\frac{dW}{dt} = \lambda SV + I(a\overline{W} - c\overline{W}^2) - \epsilon \overline{W} m_I I. \tag{4}$$

Notice that $-\lambda SV$ and $\epsilon \overline{W} m_I I$ appear with reversed signs in the equation of W as $V + W$ is the total number of viruses and does not change due to infection processes but only by replication. Choosing a logistic growth term $I(a\overline{W} - c\overline{W}^2)$, we again assume that confined viruses are distributed uniformly over the hosts and that the same logistic growth law with maximum growth rate a and competition parameter c holds in every single host cell. Thus, we can simply multiply the logistic reproduction term in each host cell by I and obtain the total number of reproduced

viruses. So, by substituting (2) for $\overline{W}$, the model takes the form

$$\begin{aligned}
\frac{dV}{dt} &= -\lambda SV - m_V V + \epsilon m_I W, \\
\frac{dW}{dt} &= aW - c\frac{W^2}{I} - \epsilon m_I W + \lambda SV, \\
\frac{dS}{dt} &= rS\left(1 - \frac{S+I}{K}\right) - \lambda SV, \\
\frac{dI}{dt} &= \lambda SV - m_I I.
\end{aligned} \tag{5}$$

A scheme of the original model and the extension is shown in Figure 1. Finally, we adimensionalize the above model by means of the following substitutions:

$$v = \frac{V}{K},\ w = \frac{W}{K},\ s = \frac{S}{K},\ i = \frac{I}{K},\ \tau = \lambda K t$$

and dimensionless parameters

$$\nu := \frac{m_V}{\lambda K},\ \mu := \frac{m_I}{\lambda K},\ \rho := \frac{r}{\lambda K}\ A := \frac{a}{\lambda K},\ \theta := \frac{c}{\lambda K}$$

to get

$$\frac{dv}{d\tau} = -sv - \nu v + \epsilon\mu w =: f_V, \tag{6}$$

$$\frac{dw}{d\tau} = sv + (A - \epsilon\mu)w - \theta\frac{w^2}{i} =: f_W, \tag{7}$$

$$\frac{ds}{d\tau} = -sv + \rho s[1 - (s+i)] =: f_S, \tag{8}$$

$$\frac{di}{d\tau} = sv - \mu i =: f_I. \tag{9}$$

3. **Analysis of the local model.** The interior equilibrium of the model is computed and its stability is analysed. Due to the singularity $\frac{w^2}{i}$ in (9), boundary equilibria are hard to analyse. The results of the analysis are summarised in Figure 2.

3.1. **Removing the singularity.** The singularity in (7) can be removed by choosing new variables $\tilde{v} := \frac{v}{i}$ and $\tilde{w} := \frac{w}{i}$. Differentiating $\tilde{v}$ with respect to t leads to

$$\tilde{v}'(t) = \frac{v'(t)}{i(t)} - \tilde{v}(t)\frac{i'(t)}{i(t)} = \frac{f_V}{i} - \tilde{v}\,\frac{f_I}{i}.$$

By using (6) and (9), the equation for the transformed variable can be calculated:

$$\begin{aligned}
\frac{d\tilde{v}}{dt} =& \frac{f_V}{i} - \tilde{v}\,\frac{f_I}{i} \\
=& -s\tilde{v} - \nu\tilde{v} + \epsilon\mu\tilde{w} - \tilde{v}\,(s\tilde{v} - \mu) \\
=& -s\tilde{v}(1+\tilde{v}) + (\mu - \nu)\tilde{v} + \epsilon\mu\tilde{w}.
\end{aligned} \tag{10}$$

The equation for $\tilde{w}$ is found by an analogous computation:

$$\frac{d\tilde{w}}{dt} = s\tilde{v}(1-\tilde{w}) + A\tilde{w} - \theta\tilde{w}^2 + \mu\tilde{w}(1-\epsilon). \tag{11}$$

In the equations for s and i, only v has to be replaced by $\tilde{v}i$. In the transformed system the equations describing the virus population and the equations of the host

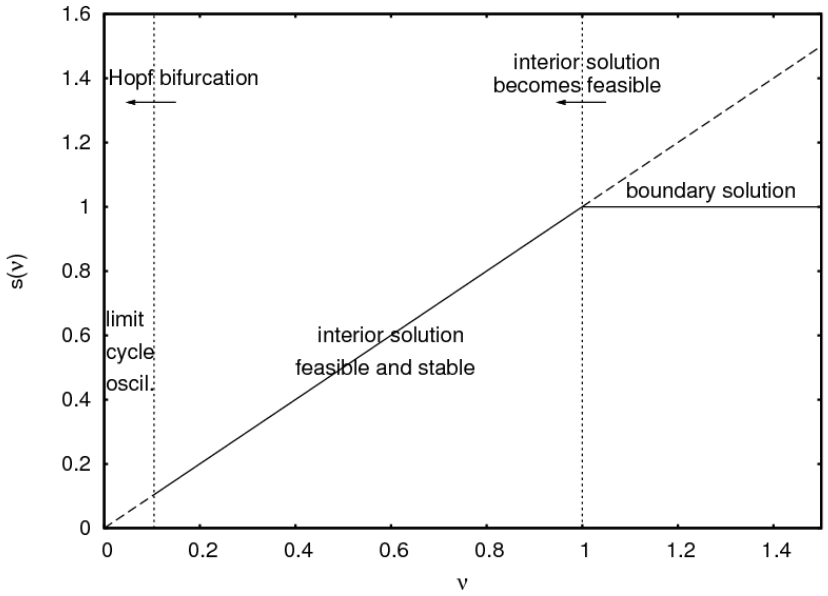

FIGURE 2. For decreasing ν, the boundary equilibrium with extinction of the infection passes over to a coexistence solution. After further decreasing ν, the coexistence solution is destabilised by a Hopf bifurcation which leads to limit cycle oscillations.

populations are nearly decoupled, which makes the stability analysis difficult. However, it is necessary to pass over to this form as a stability analysis of the singular system is impossible.

3.2. **Extinction of all species.** Already this case is quite complicated: setting $s = 0$ in (10) and (11) leads to two stationary solutions, $\tilde{v} = \tilde{w} = 0$ and a positive solution. Fortunately, independently of the values for $\tilde{v}$ and $\tilde{w}$, the Jacobian has the positive eigenvalue ρ, so that the stability of this solution can be excluded.

3.3. **Extinction of the infection.** The stability of this case, however, is hard to analyse. Although the virus population vanishes, the variables $\tilde{v}$ and $\tilde{w}$ usually have positive values. This counter-intuitive effect results from the singularity w^2/i in the original equations.

Nevertheless it can be shown that extinction of the infection is stable if

$$\tilde{v} < \mu, \tag{12}$$

$$\tilde{w} < 1 + \nu, \tag{13}$$

which—as will be seen later—implies that the interior stationary solution becomes unstable. To see this, we first compute the Jacobian of the transformed system (10), (11) where in (8) and (9) sv is replaced by $si\tilde{v}$. The Jacobian $J_{(\tilde{v},\tilde{w},1,0)}$

reads

$$J_{(\tilde{v},\tilde{w},1,0)} = \begin{pmatrix} -1+\mu-\nu-2\tilde{v} & \epsilon\mu & -\tilde{v}(1+\tilde{v}) & 0 \\ 1-\tilde{w} & A-\tilde{v}-2\theta\tilde{w}+\mu(1-\epsilon) & \tilde{v}(1-\tilde{w}) & 0 \\ 0 & 0 & -\rho & -\rho-\tilde{v} \\ 0 & 0 & 0 & -\mu+\tilde{v} \end{pmatrix}. \tag{14}$$

This matrix has one negative eigenvalue, $-\rho$, and gives the condition $\tilde{v} < \mu$. The remaining submatrix in the upper left can be shown to have only negative eigenvalues. By using (10) for substituting $-1+\mu-\nu$ by $\tilde{v}-\epsilon\mu\dfrac{\tilde{w}}{\tilde{v}}$, the upper left component becomes $-\epsilon\mu\dfrac{\tilde{w}}{\tilde{v}}-\tilde{v}$, which is clearly negative for positive values of $\tilde{v}$ and $\tilde{w}$. Analogously, by replacement of $\tilde{v}+2\theta\tilde{w}$ using (11), the other element of the diagonal also can be shown to be negative. Thus, the trace of the matrix is negative, because both summands are negative. Direct computation of the determinant—using the simplified components of the Jacobian—leads to

$$\operatorname{Det} J_{(\tilde{v},\tilde{w},1,0)} = \frac{\tilde{v}^2}{\tilde{w}} + \epsilon\mu\tilde{w} + \theta\tilde{v}\tilde{w} + \epsilon\mu\theta\frac{\tilde{w}^2}{\tilde{v}},$$

which is positive so that stability follows.

It remains to show (13), which can be done by solving (10) for $\tilde{w}$:

$$\tilde{w} = \frac{(\tilde{v}-\mu)+1+\nu}{\epsilon\mu}\tilde{v}. \tag{15}$$

From (15) one can deduce that if $\tilde{v} < \mu$, holds $\tilde{w} < 1+\nu$ also is fulfilled.

3.4. **Interior stationary solution.** The interior stationary solution of the model is computed explicitly. If we take $s \neq 0$ in (8) and use (9), we find $v = \rho(1-i-s) = \mu\dfrac{i}{s}$, from which

$$i = \rho\frac{(1-s)s}{\mu+\rho s}. \tag{16}$$

Again with (8) and (9) we obtain

$$v = \mu\frac{i}{s}. \tag{17}$$

Also (6), (8), and (9) combined give $-\nu\mu\dfrac{i}{s} + \mu(\epsilon w - i) = 0$, which leads to

$$w = \frac{i}{\epsilon}\left(1+\frac{\nu}{s}\right). \tag{18}$$

By substituting for w, i, and s in (7), s can be computed. By substituting μi for sv and using (18), the equation $f_W = 0$ can be simplified to the form

$$\frac{i}{\epsilon}\left\{\epsilon\mu + \left(1+\frac{\nu}{s}\right)\left[A-\epsilon\mu-\frac{\theta}{\epsilon}\left(1+\frac{\nu}{s}\right)\right]\right\} = 0. \tag{19}$$

By factoring out $1/s^2$, (19) is transformed to the quadratic equation in s,

$$\epsilon\mu s^2 + (s+\nu)\left[(A-\epsilon\mu)s - \frac{\theta}{\epsilon}(s+\nu)\right] = 0 \tag{20}$$

which simplifies to

$$\left(A-\frac{\theta}{\epsilon}\right)s^2 + \nu\left(A-\epsilon\mu-2\frac{\theta}{\epsilon}\right)s - \frac{\theta}{\epsilon}\nu^2 = 0. \tag{21}$$

This shows that for calculating the stationary solution s, the parameter ϵ only leads to a different scaling of the virulence μ and the competition parameter θ. We therefore define

$$\bar{\mu} := \epsilon\mu,\ \bar{\theta} = \frac{\theta}{\epsilon}. \tag{22}$$

These new parameters have a clear biological significance: increased values of ϵ on the one hand accelerate the release of viruses, and on the other hand the importance of intraspecific competition of viruses inside the host cells is decreased. The solutions of (19) are

$$s_{1,2} = \frac{\nu}{2(A-\bar{\theta})}\left(\bar{\mu} + 2\bar{\theta} - A \pm \sqrt{(\bar{\mu}-A)^2 + 4\bar{\theta}\bar{\mu}}\right). \tag{23}$$

3.5. **Feasibility conditions for the interior solution.** In this section, starting from $0 < s < 1$ it will be shown that only the branch s_1 of (23) is feasible. Under the condition which is obtained by solving $s_1 \geq 1$ for ν,

$$\nu \geq \nu_{max} = \frac{1}{2\bar{\theta}}\left(A - 2\bar{\theta} - \bar{\mu} + \sqrt{(A - m\bar{u})^2 + 4\bar{\theta}\bar{\mu}}\right), \tag{24}$$

the interior solution is infeasible. In this case the infection goes extinct (see Section 3.6).

3.5.1. *Feasible branch.* Assuming $A > \bar{\theta}$ we need to show that

$$\bar{\mu} + 2\bar{\theta} - A + \sqrt{(\bar{\mu}-A)^2 + 4\bar{\theta}\bar{\mu}} > 0,$$

which is always true as

$$\sqrt{(\bar{\mu}-A)^2 + 4\bar{\theta}\bar{\mu}} > |\bar{\mu} - A|.$$

From this result it is also immediately clear that s_1 is negative if $A < \bar{\theta}$. So $A > \bar{\theta}$ is a necessary and sufficient condition for s_1 to be positive.

3.5.2. *Infeasible branch.* It is easy to show that the other branch s_2 of (23) can never occur, because it is always negative. Assuming again $A > \bar{\theta}$, we need to verify whether the following inequality holds

$$-2(A-\bar{\theta}) + \bar{\mu} + A > \sqrt{(\bar{\mu}+A)^2 - 4\bar{\mu}(A-\bar{\theta})}.$$

A contradiction would immediately arise if the left-hand side were negative, so without loss of generality, both sides of the inequality can be regarded as positive. Thus, squaring both sides and dividing by $4(A-\bar{\theta})$ we find

$$(\bar{\mu}+A)^2 - 4(A-\bar{\theta})(\bar{\mu}+A) + 4(A-\bar{\theta})^2 > (\bar{\mu}+A)^2 - 4(A-\bar{\theta})\bar{\mu},$$

which implies

$$-(\bar{\mu}+A) + (A-\bar{\theta}) > -\bar{\mu},$$

thus finally reaching the contradiction $\bar{\theta} < 0$. Conversely, for $A < \bar{\theta}$, $A - 2\bar{\theta} - \bar{\mu}$ is negative, so the whole expression must be negative.

3.6. **Stability of the interior stationary solution.** Stability of the interior stationary solution is analysed by the Routh-Hurwitz criterion; see for example, [7]. Choosing ν, the mortality rate of viruses, as a bifurcation parameter, it can be shown that as ν is decreased, the interior solution "collides" with the boundary solution $s^* = 1$ for a value $\nu = \nu_{max}$. For $\nu < \nu_{max}$ the interior solution becomes stable and $s^* = 1$ loses stability. By further decreasing ν a Hopf bifurcation again destabilizes the interior solution which leads to limit cycle oscillations (see Section 4).

3.6.1. *Simplification of the Jacobian at the interior stationary solution.* The Jacobian J can be simplified by using (6-9) and (16-18). Solving $f_W = 0$, (see (7)) for A, again applying the definition (22),

$$A = \bar{\mu} - s\frac{v}{w} + \theta\frac{w}{i},$$

is obtained. Substituting for A in J_{22} leads to

$$J_{22} = -s\frac{v}{w} - \theta\frac{w}{i} = -\mu\frac{i}{w} - \theta\frac{w}{i}. \tag{25}$$

One last simplification can be found for $J_{33} = \rho(1 - i - 2s) - v$. From (8) it can easily be seen that $\rho(1 - i - s) = v$; thus we simply obtain

$$J_{33} = -\rho s. \tag{26}$$

Putting our results (25–26) together, a simplified Jacobian $\tilde{J}$ is obtained:

$$\tilde{J} = \begin{pmatrix} -\epsilon s\frac{w}{i} & \bar{\mu} & -v & 0 \\ s & -\mu\frac{i}{w} - \theta\frac{w}{i} & v & \theta\left(\frac{w}{i}\right)^2 \\ -s & 0 & -\rho s & -\rho s \\ s & 0 & v & -\mu \end{pmatrix}. \tag{27}$$

3.6.2. *Coefficients of the characteristic polynomial.* It is possible to calculate the coefficients of the characteristic polynomial

$$q(X) = \sum_{k=0}^{n} a_k X^k \tag{28}$$

directly from $\tilde{J}$ as a_k can be calculated by the following formula using the principal minors of order i:

$$a_i = (-1)^i \sum_{R \subset A_i} M_R, \quad i = 0, ..., 3. \tag{29}$$

Here A_i denote the subsets of $\{1, ..., 4\}$ consisting of i elements. The principal minors are determinants of submatrices which are obtained by deleting $0, 1..., (n-1)$ rows and the corresponding columns of the matrix $\tilde{J}$.

Rather lengthy computations lead to the following expressions of the coefficients $a_0, ..., a_3$:

$$\begin{aligned} a_0(\nu) &= \frac{\mu i^2 + \theta w^2}{i^2 w}(\epsilon w - i)(\mu + \rho s)sv \\ &= \frac{\rho\mu\nu[\bar{\mu}s^2 + \bar{\theta}(\nu + s)^2](1 - s)}{s(\nu + s)} \end{aligned} \tag{30}$$

$$\begin{aligned} a_1(\nu) &= \bar{\theta}(s + \nu)\{\rho[(s + \nu) + \mu + v] - v\} + \frac{\bar{\mu}s^2[\rho\mu + (\rho - 1)v]}{s + \nu} \\ &+ \rho\nu s(s + \nu)v + \mu s[\rho(s + \nu) + (\epsilon - 1)v] \end{aligned} \tag{31}$$

$$\begin{aligned} a_2(\nu) &= s[\rho\mu + (\rho - 1)v] + \bar{\mu}(\mu + \rho s)\frac{s}{s + \nu} \\ &+ \bar{\theta}\frac{(s + \nu)^2}{s} + (s + \nu)(\mu + \rho s)\left(1 + \frac{\bar{\theta}}{s}\right) \end{aligned} \tag{32}$$

$$a_3(\nu) = \frac{(\nu + s)^2(s + \bar{\theta}) + (\nu + s)s(\mu + \rho s) + \bar{\mu}s^2}{s(\nu + s)}. \tag{33}$$

The coefficients have been written as functions of ν, since stability will be investigated in terms of the latter parameter. It is immediately seen that a_3 is positive for all parametrisations. Then, a_0 is positive provided that $s \in]0, 1[$. This indicates that the interior stationary solution loses stability as soon as it becomes infeasible. If the additional condition $\rho \geq 1$ is imposed, a_1 and a_2 are positive. Two additional stability conditions must be fulfilled by the Routh-Hurwitz criterion. These are investigated in the next section.

4. **The Hopf bifurcation.** We now analyse the possibility that the equilibrium E_* bifurcates. For this to occur, we must have that the characteristic polynomial factors as follows

$$\Lambda(\sigma) = (\sigma^2 + p^2)(\sigma^2 + q\sigma + r),$$

with

$$q = a_3, \quad r = \frac{a_0 a_3}{a_1}, \quad p = \sqrt{\frac{a_1}{a_3}}.$$

Therefore a Hopf bifurcation occurs if the following condition holds:

$$a_1(\nu_H)a_2(\nu_H)a_3(\nu_H) = a_1^2(\nu_H) + a_0(\nu_H)a_3^2(\nu_H) \tag{34}$$

at the Hopf bifurcation point $\nu = \nu_H$. According to [4] the additional condition

$$a_1(\nu_H)a_2(\nu_H) - a_0(\nu_H)a_3(\nu_H) > 0 \tag{35}$$

must hold. We define

$$q_1(\nu) := a_1(\nu)a_2(\nu)a_3(\nu) \tag{36}$$

$$q_2(\nu) := a_1^2(\nu) + a_0(\nu)a_3^2(\nu). \tag{37}$$

The condition

$$\left.\frac{d(q_1(\nu) - q_2(\nu))}{d\nu}\right|_{\nu=\nu_H} \neq 0 \tag{38}$$

ensures that at the bifurcation point the real part of the eigenvalues changes sign. For details, [4] may be consulted.

4.1. **Outline of the proof.** As the coefficients of the characteristic polynomial are complicated, the necessary calculations cannot be carried out explicitly. Thus, (34) is proven by showing the existence of an intersection of $q_1(\nu)$ and $q_2(\nu)$. The proof leans mostly on monotonicity of $q_1(\nu)$. It is simplified by the fact that the feasible range of the susceptibles s is $[0, 1]$, or $\nu \in [0, \nu_{max}]$. In Section 4.2 it is shown that both $q_1(\nu)$ and $q_2(\nu)$ tend to zero as ν tends to zero. As q_1 and q_2 are rational functions of ν with q_1 having a higher total degree than q_2, they can intersect only if the derivative $q_1'(0)$ is smaller than $q_2'(0)$. The derivatives are computed in Section 4.3, this leads to the necessary condition (50) for the Hopf bifurcation. As q_1 is always strictly greater than q_2 at the right end of the feasible range at $\nu = \nu_{max}$, which is shown in 4.4, it suffices to demonstrate that q_1 inreases monotonically in the feasible interval $[0, \nu_{max}]$, as shown in 4.5 under the additional condition $\rho \geq 1$. Under this assumption, the additional constraint (35) also is proven. In Figure 3, a sketch of $q_1(\nu)$ and $q_2(\nu)$ is given as proven in Sections 4.2-4.5.

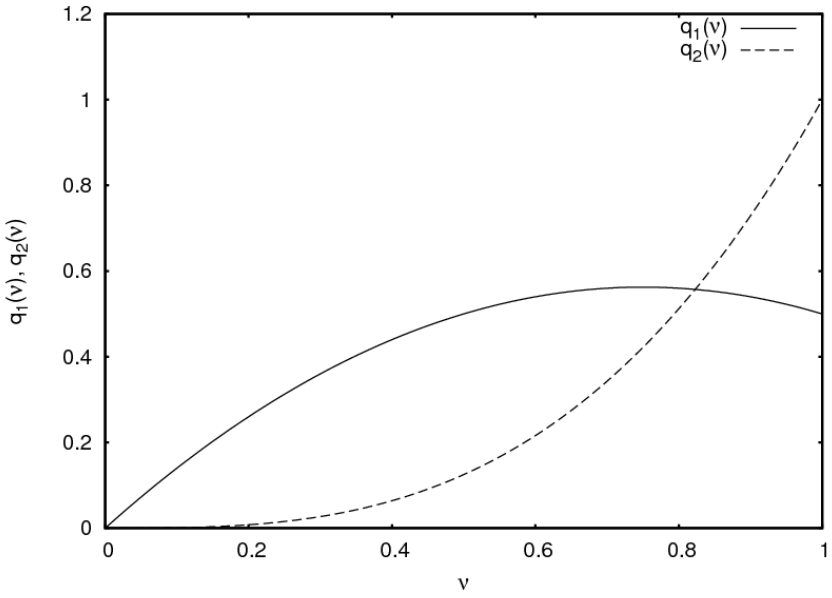

FIGURE 3. The relative position of $q_1(\nu)$ and $q_2(\nu)$ as proven in Sections 4.2-4.5.

4.2. **Coefficients behaviour for $\nu \to 0$.** As s depends linearly on ν, it is possible to factor out ν at every s. Thus, it is easily seen that in (30) and (31), one ν remains in the numerator after cancelling out, so that the limit $\nu \to 0$ exists and is 0.

In the following, factoring out of ν is expressed explicitly by

$$s := \frac{\nu}{\nu_{max}} \tag{39}$$

where ν_{max} depends on A, μ, and θ (cf. (24)) and, for simplifying the representation of the results,

$$\zeta := \frac{\bar{\mu} + \bar{\theta}(1 + \nu_{max})^2}{1 + \nu_{max}}. \tag{40}$$

In a_2, the terms $(\nu+s)^2\theta$ and $\mu^2 s^2$ have the same degree in ν as the denominator $s(\nu+s)$. Therefore a_2 tends to a nonzero constant for $\nu \to 0$:

$$\lim_{\nu\to 0} a_2(\nu) = \mu\,\frac{\bar{\mu}+\bar{\theta}(1+\nu_{max})^2}{1+\nu_{max}} = \mu\,\zeta. \tag{41}$$

With (39) also the limit of a_3 can be calculated:

$$\lim_{\nu\to 0} a_3(\nu) = \bar{\theta}\,(1+\nu_{max}) + \mu + \frac{\bar{\mu}}{1+\nu_{max}} \tag{42}$$

$$= \frac{\bar{\theta}(1+\nu_{max})^2 + \bar{\mu} + \mu(1+\nu_{max})}{1+\nu_{max}} = \zeta + \mu. \tag{43}$$

As all limits exist for $\nu \to 0$, the limits of $a_1a_2a_3$ and $a_1^2 + a_0a_3^2$ also exist. Both limits are 0.

4.3. **Comparison of derivatives for $\nu \to 0$.** The idea of proving the existence of a Hopf bifurcation leans on the total degrees of q_1 and q_2 as rational functions: q_1 having a total degree of 5 increases faster for $\nu \to \infty$ than q_2 having a smaller total degree. Because both curves intersect at $\nu = 0$, it depends on the derivative at 0 which of the curves will be "below" for small positive values of ν. Only if q_1, the curve with the higher total degree, is "below" the other one, there will be an intersection. Thus, the derivatives of q_1 and q_2 with respect to ν will be compared. For $q_1'(0)$ we find

$$\begin{aligned} q_1'(0) &= a_1'(0)a_2(0)a_3(0) + a_1(0)a_2'(0)a_3(0) + a_1(0)a_2(0)a_3'(0) \\ &= a_1'(0)a_2(0)a_3(0). \end{aligned} \tag{44}$$

as a_1 has a zero at $\nu = 0$. As also a_0 has a zero for $\nu \to 0$, $q_2'(0)$ simplifies:

$$\begin{aligned} q_2'(0) &= 2a_1'(0)a_1(0) + a_0'(0)a_3(0)^2 + 2a_0(0)a_3'(0)a_3(0) \\ &= a_0'(0)a_3^2(0). \end{aligned} \tag{45}$$

Thus, only $a_0'(0)$ and $a_1'(0)$ have to be calculated:

$$a_0'(0) = \rho\mu\frac{\bar{\mu}+\bar{\theta}(1+\nu_{max})^2}{1+\nu_{max}} = \rho\mu\zeta \tag{46}$$

$$\begin{aligned} a_1'(0) &= \rho\frac{(\rho-1+\mu)[\bar{\mu}+\bar{\theta}(1+\nu_{max})^2] + \mu(\epsilon-1)(1+\nu_{max})}{\nu_{max}(1+\nu_{max})} \\ &= \frac{\rho}{\nu_{max}}[(\rho-1+\mu)\zeta + \rho\mu(\epsilon-1)]. \end{aligned} \tag{47}$$

The comparison of $q_1'(0)$ and $q_2'(0)$ is done by comparing the quotient with 1:

$$\begin{aligned} \frac{q_1'(0)}{q_2'(0)} &= \frac{a_1'(0)a_2(0)}{a_0'(0)a_3(0)} \\ &= \frac{\frac{\rho}{\nu_{max}}[(\rho-1+\mu)\zeta + \rho\mu(\epsilon-1)]\,\mu\zeta}{\rho\mu\zeta(\zeta+\mu)} \\ &= \frac{(\rho-1+\mu)\zeta + \rho\mu(\epsilon-1)}{\nu_{max}(\zeta+\mu)} < 1. \end{aligned} \tag{48}$$

This can be used to compute an upper bound for ρ:

$$\rho < \frac{\mu(\nu_{max}-\zeta) + (1+\nu_{max})\zeta}{(\epsilon-1)\mu + \zeta}, \tag{49}$$

which for the special case $\epsilon = 1$ gives

$$\rho < 1 + \nu_{max} + \frac{1 + \nu_{max}}{1 + \frac{\theta}{\mu}(1 + \nu_{max})^2}\nu_{max} - \mu. \tag{50}$$

4.4. **Behaviour of q_1 and q_2 at the right end of the feasible range.** Now that a condition for an intersection has been obtained, it will be demonstrated that $q_1(\nu_{max})$ is always greater than $q_2(\nu_{max})$. This ensures that the Hopf bifurcation always occurs for a value ν_H in the feasible range $]0, \nu_{max}]$; i.e. there is always a nonempty interval $]\nu_H, \nu_{max}]$ where the interior stationary solution is stable.

As a_0 has a zero at $s(\nu_{max}) = 1$, $q_2(\nu_{max}) = (a_1(\nu_{max}))^2$. This makes it easy to compare q_1 and q_2 at this value; only

$$a_2(\nu_{max})\, a_3(\nu_{max}) > a_1(\nu_{max}) \tag{51}$$

has to be checked. The calculations are simplified a little, since $\nu = \nu_{max}$ implies $s = 1$ and $v = 0$. The results for a_1 and a_2 are

$$a_1(\nu_{max}) = \rho\,\bar{\theta}(1 + \nu_{max})[(1 + \nu_{max}) + \mu] + \rho\mu\left[(1 + \nu_{max}) + \frac{\bar{\mu}}{1 + \nu_{max}}\right], \tag{52}$$

$$\begin{aligned} a_2(\nu_{max}) &= \rho\mu + \bar{\mu}\frac{\mu + \rho}{1 + \nu_{max}} + \bar{\theta}(1 + \nu_{max})[(1 + \nu_{max}) + \mu] \\ &\quad + (1 + \nu_{max})\mu + \rho(1 + \bar{\theta})(1 + \nu_{max}) \\ &= \frac{a_1(\nu_{max})}{\rho} + \rho\left((1 + \bar{\theta})(1 + \nu_{max}) + \mu + \frac{\bar{\mu}}{1 + \nu_{max}}\right). \end{aligned} \tag{53}$$

Evaluating a_3 at ν_{max}

$$a_3(\nu_{max}) = \rho + \mu + (1 + \nu_{max})(1 + \bar{\theta}) + \frac{\bar{\mu}}{1 + \nu_{max}}, \tag{54}$$

we notice that $a_3(\nu_{max})$ contains ρ and other positive summands, which proves that (51) is true.

4.5. **Rigorous proof for $\rho \geq 1$.** For the remainder, in addition to (50), $\rho \geq 1$ will be assumed. Under these conditions the existence of a Hopf bifurcation can be proven rigorously. However, although for $\rho < 1$ it is even easier to satisfy (50) it is technically more difficult to show that (35) and (38) are met.

Notice that $q_1(\nu)$ and $q_2(\nu)$ have only negative poles; furthermore, the numerator of $q_1(\nu)$ has only positive coefficients. Thus, $q_1(\nu)$ is monotonically increasing for positive values of ν. This ensures that the intersection of $q_1(\nu)$ and $q_2(\nu)$ is unique and transversal, so that (34) and (38) are satisfied.

Finally, we note that for $\rho \geq 1$, (34) implies (35): We have already shown that a_1, a_2, and a_3 are positive for positive values of ν. At ν_H where $a_1 a_2 a_3$ and $a_1^2 + a_0 a_3^2$ meet dividing by a_3 leads to

$$a_1(\nu_H)a_2(\nu_H) = \frac{a_1^2(\nu_H)}{a_3(\nu_H)} + a_0(\nu_H)a_3(\nu_H) > a_0(\nu_H)a_3(\nu_H)$$

as all summands are positive. Thus, the occurence of a Hopf bifurcation is proven under the additional constraints (50) and $\rho \geq 1$.

5. **The spatial model.** In contrast to other population models, the transition to the spatial model is not completely straightforward in this case. The fact that viruses which are inside their hosts cannot move by themselves but are merely transported by the infected cells in which they are confined must be taken into account. To make the solution chosen here more plausible, consider the following diffusion equations without reaction terms:

$$\frac{\partial w}{\partial t} = \frac{w}{i} D\Delta i, \tag{55}$$

$$\frac{\partial i}{\partial t} = D\Delta i. \tag{56}$$

The diffusive flow of i is converted into w by the proportional factor $\frac{w}{i}$. By substituting for $D\Delta i$ in the equation (55), this equation is reduced to an ordinary differential equation in w and i:

$$\frac{dw}{dt} = \frac{w}{i}\frac{di}{dt}, \quad w(0) = w_0,\ i(0) = i_0.$$

The equation can be easily solved by separation of variables by

$$w(t) = \frac{w_0}{i_0}\, i(t).$$

This is the desired result: The ratio of $w(t)$ and $i(t)$ is conserved only if transport is considered.

Thus, the equations of the reaction-diffusion system are (see (6–9)):

$$\frac{\partial v}{\partial \tau} = f_V + D\Delta v, \tag{57}$$

$$\frac{dw}{d\tau} = f_W + \frac{w}{i} D\Delta i, \tag{58}$$

$$\frac{ds}{d\tau} = f_S + D\Delta s, \tag{59}$$

$$\frac{di}{d\tau} = f_I + D\Delta i. \tag{60}$$

Solutions for the representative sample parametrisation,

$$\begin{aligned} &\rho = 10,\ \nu = 14.925,\ \mu = 24.628, \\ &A = 40,\ \theta = 0.21,\ \epsilon = 1,\ D = 0.05, \end{aligned} \tag{61}$$

are presented in Figure 4.

6. **Conclusions.** The complete viral life cycle, including the relevant processes from infection by replication in host cells to lysis of the hosts and release of replicated viral particles, could be represented in a surprisingly simple model. The model's behaviour is structurally very similar to the model by Beretta and Kuang [1], on which it is based: decreasing ν (i.e. increasing the strength of the infection) leads to a transition from extinction of the infection for high values of ν through equilibrium levels of all populations to limit cycle oscillations. This corresponds to the behaviour of the model presented in [1] if the viral replication factor B is increased. Thus, the extension allows for a deeper insight into the dependence of the replication factor B on the logistic growth parameters A and θ of confined viruses and the mortality of infected μ; i.e., in fact, the dependence of B on the crucial parameters of the infection. In this section we restrict our considerations to the case $\epsilon = 1$.

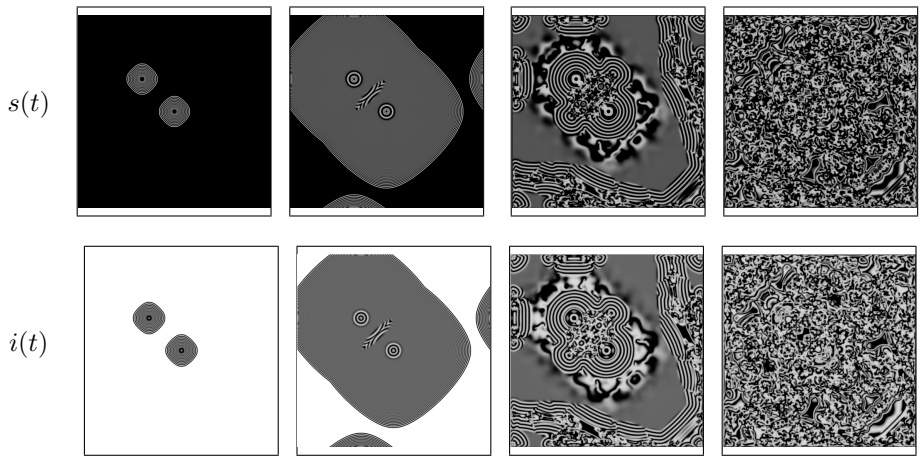

(a) $t = 10$ (b) $t = 50$ (c) $t = 200$ (d) $t = 300$

FIGURE 4. Simulation of the spatial model for parametrisation (61) with periodic boundary conditions. Only the solutions for susceptible and infected phytoplankton are given. The higher the densities of a population, the darker are the gray values which are used for painting it. Initial conditions: the whole space is covered with a homogeneous distribution of phytoplankton, two square patches of viruses. First, infected expand in concentric circles ($t = 10$) which are transformed in a homogeneous distribution by dynamic stabilisation, [6], ($t = 50$). Afterwards, small spiral waves form in the center, and suddenly more extended structures start from the center and quickly reach the boundary ($t = 200$). Finally, all bigger structures dissolve and only small patterns remain ($t = 300$).

First, looking at (18) the ratio

$$\begin{aligned} B_\infty := \frac{w}{i} &= 1 + \frac{\nu}{s} = 1 + \nu_{max} \\ &= \frac{1}{2}\left(\frac{A}{\theta} - \frac{\mu}{\theta}\right) + \sqrt{\frac{1}{4}\left(\frac{A}{\theta} - \frac{\mu}{\theta}\right)^2 + \frac{\mu}{\theta}} \end{aligned} \tag{62}$$

can be computed. As pointed out in Section 2, we have replaced B by $\frac{w}{i}$ in the model equations, assuming that at lysis the average amount of confined viruses per cell is set free. B_∞ can be understood as the average amount of viruses which is set free if the stationary solution is attained; i.e., for $t \to \infty$.

From (62), it immediately follows that the stability condition $B > 1 + \nu$ from the original model remains valid in the extended model:

$$B_\infty = 1 + \nu_{max} > 1 + \nu \tag{63}$$

as $\nu < \nu_{max}$ is the feasibility condition for the interior stationary solution.

Furthermore, (62) allows us to compare parameter sets of the Beretta-Kuang model [1], with the extension: having fixed B and μ by a previous run of the original model, a relationship between the logistic growth parameters A and θ for

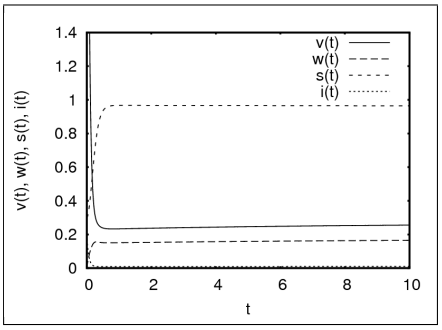

(b) extended model, $A = 27.26$, $\theta = 0.25$

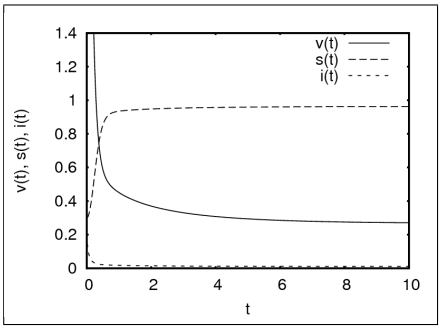

(a) Beretta/Kuang model, $B = 16.5$

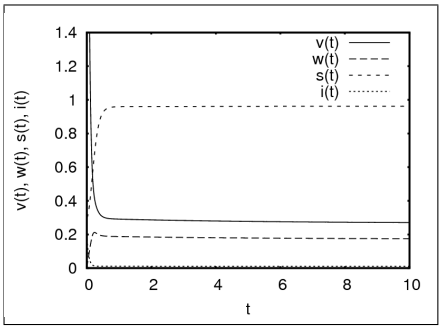

(c) extended model, $A = 31.39$, $\theta = 0.5$

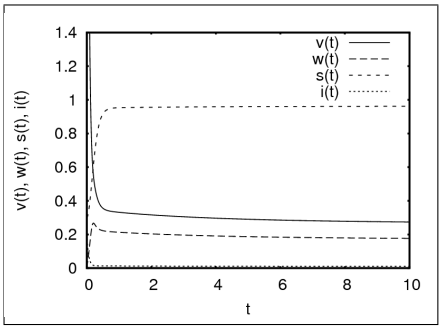

(d) extended model, $A = 35.51$, $\theta = 0.75$

FIGURE 5. The original model (see [1]) with the replication factor $B = 16.5$ is compared with the extended model for different choices of A and θ.

confined viruses can be computed. Solving for θ leads to

$$\theta = \frac{1}{B_\infty}\left[A - \mu\left(1 - \frac{1}{4B_\infty}\right)\right]$$

which shows that there is a lower bound for the growth rate of viruses

$$A_{min} = \mu\left(1 - \frac{1}{4B_\infty}\right). \tag{64}$$

A must have values strictly above A_{min}, because choosing $\theta = 0$ leads to unrealistic solutions: if no intraspecific competition of viruses is considered, for some parametrisations, the hosts may go extinct and viruses prevail. Taking into account that B ranges from 10 to 100, it can be assumed that A_{min} corresponds to μ.

As an example, the parameter values proposed in [1] are chosen and the Hopf bifurcation points are computed numerically for both models:

$$\rho = 10,\ \nu = 14.925,\ \mu = 24.628. \tag{65}$$

Numerical solutions with $B = 16.5$ and three corresponding parameter sets of the extended model are shown in Figure 5. For the original model, the Hopf bifurcation occurs at $B \approx 94.45$, whereas in the extended model the value $B_\infty \approx 80.70$ is found. Also, frequency and amplitude of the periodic solutions cannot be adjusted simultaneously by appropiate choices of A and θ; see Figure 6.

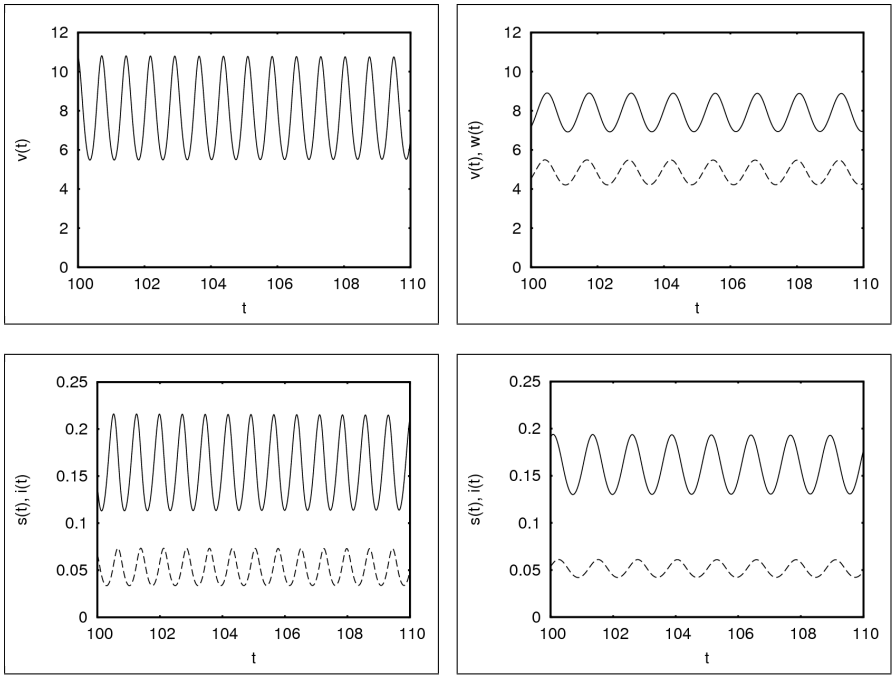

(a) Beretta-Kuang model $B = 95$ (b) extended model, $A = 29.12$, $\theta = 0.05$

FIGURE 6. The original model (see [1]) with the replication factor $B = 95$; i.e., for B above the Hopf bifurcation point, is compared with the extended model. Frequency and amplitude of the periodic solutions cannot be adjusted simultaneously by appropriate choices of A and θ.

The discovered relationship of the extension to the original model on the one hand suggests that the extension is indeed plausible. On the other hand the extended model can give insight in the replication of viruses which are replicating in their hosts, even providing means for determining the growth rate and the competition parameter of the viruses. As these parameters seem inaccessible by empirical investigations this gives a good example for the power of mathematical modelisation.

Acknowledgements. I. S. thanks Michel Langlais for insisting on the importance of removing the singularity in the model. The authors are grateful for the helpful suggestions by Edoardo Beretta, which greatly improved the article. All authors acknowledge the financial support by the VIGONI program, which very much facilitated the cooperation.

REFERENCES

[1] Beretta, E. and Kuang, Y. (1998). Modeling and analysis of a marine bacteriophage infection. *Mathematical Biosciences* **149**: 57–76.

[2] Hilker, F. M. and Malchow, H. (2006). Strange periodic attractors in a prey-predator system with infected prey. *Mathematical Population Studies* **13**: 119–34.

[3] Hilker, F. M., Malchow, H., Langlais, M., and Petrovskii, S. V. (2006). Oscillations and waves in a virally infected plankton system. Part II: Transition from lysogeny to lysis. *Ecological Complexity* **3**: 200–08.

[4] Liu, W.-M. (1994).Criterion of Hopf bifurcations without using eigenvalues. *Journal of Mathematical Analysis and Applications* **182**: 250–56.

[5] Malchow, H., Hilker, F. M., Petrovskii, S. V., and Brauer, K. (2004). Oscillations and waves in a virally infected plankton system. Part I: The lysogenic stage. *Ecological Complexity* **1**: 211–23.

[6] Malchow, H. and Petrovskii, S. V. (2002). Dynamical stabilization of an unstable equilibrium in chemical and biological systems. *Mathematical and Computer Modelling* **36**: 307–19.

[7] Murray, J. D. (2002). *Mathematical biology. I. An introduction*, volume 17 of *Interdisciplinary Applied Matthematics*. Berlin: Springer.

[8] Siekmann, I., Malchow, H., and Venturino, E. (2007). Predation may defeat spatial spread of infection. *Journal of Biological Dynamics* **2**: 40–45.

Received on December 21, 2007. Accepted on February 27, 2008.

E-mail address: ivo.siekmann@uos.de
E-mail address: ezio.venturino@unito.it
E-mail address: malchow@uos.de